https://doi.org/10.1093/plphys/kiad372 PLANT PHYSIOLOGY 2023: 193: 1349–1364

Plant Physiology®

Research Article

Leaf hydraulic maze: Abscisic acid effects on bundle sheath, palisade, and spongy mesophyll conductance

Adi Yaaran [1], Eyal Erez,[1] Carl Procko [2] and Menachem Moshelion [1,*]

1 Institute of Plant Sciences and Genetics in Agriculture, The Robert H. Smith Faculty of Agriculture, Food and Environment, The Hebrew University of Jerusalem, Rehovot 76100, Israel
2 Plant Biology Laboratory, Salk Institute for Biological Studies, La Jolla, CA 92037, USA

*Author for correspondence: menachem.moshelion@mail.huji.ac.il
The author responsible for distribution of materials integral to the findings presented in this article in accordance with the policy described in the Instructions for Authors (https://academic.oup.com/plphys/pages/General-Instructions) is Menachem Moshelion (menachem.moshelion@mail.huji.ac.il)

Abstract

Leaf hydraulic conductance (K_{leaf}) facilitates the supply of water, enabling continual CO_2 uptake while maintaining plant water status. We hypothesized that bundle sheath and mesophyll cells play key roles in regulating the radial flow of water out of the xylem by responding to abscisic acid (ABA). Thus, we generated transgenic *Arabidopsis thaliana* plants that are insensitive to ABA in their bundle sheath (BSabi) and mesophyll (MCabi) cells. We also introduced tissue-specific fluorescent markers to distinguish between cells of the palisade mesophyll, spongy mesophyll, and bundle sheath. Both BSabi and MCabi plants showed greater K_{leaf} and transpiration under optimal conditions. MCabi plants had larger stomatal apertures, higher stomatal index, and greater vascular diameter and biomass relative to the wild-type (WT) and BSabi plants. In response to xylem-fed ABA, both transgenic and WT plants reduced their K_{leaf} and transpiration. The membrane osmotic water permeability (P_f) of the WT's spongy mesophyll was higher than that of the WT's palisade mesophyll. While the palisade mesophyll maintained a low P_f in response to high ABA, the spongy mesophyll P_f was reduced. Compared to the WT, BSabi bundle sheath cells had a higher P_f, but MCabi spongy mesophyll had an unexpected lower P_f. These results suggest that tissue-specific regulation of P_f by ABA may be confounded by whole-leaf hydraulics and transpiration. ABA increased the symplastic permeability, but its contribution to K_{leaf} was negligible. We suggest that the bundle sheath spongy mesophyll pathway dynamically responds to the fluctuations in water availability, while the palisade mesophyll serves as a hydraulic buffer.

Introduction

The movement of CO_2 into the leaf and the loss of water from the leaf both occur through the stomata, creating a strong relationship between transpiration and productivity (de Wit 1958; Fischer et al. 1998; Richards 2000; Kemanian et al. 2005; Blum 2009; Sperry et al. 2017; Sinclair 2018; Xiong and Nadal 2020). To support productivity (high transpiration), plants must efficiently conduct water from the soil to the evaporation sites in the leaf. Leaf hydraulic conductance (K_{leaf}) is a substantial bottleneck accounting for ~30% (on average) and up to 98% of the total water resistance of well-watered plants (Sack and Holbrook 2006). K_{leaf} is the ratio of water flow through the leaf (xylem to evaporation site) to the water potential gradient across the leaf (Sack and Holbrook 2006). K_{leaf} is a dynamic trait, which responds to both abiotic (Tyree et al. 2005; Blackman et al. 2009; Shatil-Cohen et al. 2011; Pou et al. 2013; Prado and Maurel 2013; Sade et al. 2015; Kelly et al. 2017) and biotic stresses (Attia et al. 2019; Dalal et al. 2020). The structural–functional regulation of leaf hydraulics involves 4 main pathways: (i) hollow xylem elements; (ii) the apoplast, along the cell walls of the leaf tissues; (iii) the symplast, which connects cells via plasmodesmata; and (iv) transmembrane transport, mainly via aquaporins (AQPs). However, little is known about the relative contributions of the different pathways and the mechanisms that regulate K_{leaf}.

A simplified approach divides K_{leaf} into 2 parts: xylem hydraulic conductance, K_x, known as the axial path, and out-of-xylem hydraulic conductance, K_{ox}, known as the radial

Received March 29, 2023. Accepted June 02, 2023. Advance access publication June 30, 2023

path. Leaf vein architecture and density greatly affect K_x (Nardini, Gortan, and Salleo 2005; Brodribb et al. 2007; Blackman et al. 2010; Brodribb et al. 2010; Scoffoni et al. 2011; Caringella et al. 2015). As the xylem vessels are composed mainly of dead cells, rapid impairment of K_{leaf} was previously attributed to breaks in the water-column continuum (i.e. embolism). However, in recent decades, research has revealed that living cells are involved in the regulation of K_{ox}, which contributes substantially to K_{leaf} and its dynamics (Shatil-Cohen et al. 2011; Sade et al. 2014; Scoffoni and Sack 2017; Grunwald et al. 2021).

The living vascular parenchyma, bundle sheath cells (BSCs) and mesophyll cells (MCs) can potentially regulate K_{ox} according to internal and environmental signals. High K_{ox} resistance may also help leaves to avoid catastrophic xylem failure (Scoffoni et al. 2017) by dynamically regulating the resistance of the "next-in-line" pathway (Yaaran and Moshelion 2016). Previously, stress-induced changes in K_{ox} were attributed to leaf shrinkage (i.e. physical alterations of the apoplastic water pathway; Scoffoni et al. 2014) and/or to changes in AQP expression and/or activity (i.e. alterations in the transmembrane water pathway). The latter has been reported in BSC (Kim and Steudle 2009; Shatil-Cohen et al. 2011; Prado et al. 2013; Sade et al. 2014), MC (Morillon and Chrispeels 2001), and guard cells (Grondin et al. 2015), as well as at the whole-leaf level (Nardini, Salleo, and Andri 2005; Cochard et al. 2007; Pou et al. 2013; Kelly et al. 2017).

The bundle sheath is a single cell layer enwrapping the vasculature, which possesses selective barrier characteristics (Pilot et al. 2004; Leegood 2008; Galvez-Valdivieso et al. 2009; Grunwald et al. 2021) with low levels of apoplastic transport (Shapira et al. 2009; Shatil-Cohen and Moshelion 2012). It is symplastically isolated from the xylem, which limits the transmembrane movement of water into the leaf, but is connected to neighboring MC by plasmodesmata (Ache et al. 2010). The anatomical structure of the MC correspondingly affects K_{leaf} (Brodribb et al. 2007; Scoffoni et al. 2014; Buckley 2015). The current assumption is that the palisade MC functions as a sort of water capacitor (Zwieniecki et al. 2007), whereas the spongy MC are more dynamic in terms of their water status and play a substantial role in the determination of K_{ox} (Buckley 2015; Xiong and Nadal 2020). In MC, water can move via all 3 pathways in parallel. A controlled trade-off between water pathways has been suggested as a mechanism for coping with drought stress (Morillon and Chrispeels 2001), yet supportive evidence for this hypothesis is scarce, and the evidence that does exist suggests routing toward the apoplastic pathway (Pou et al. 2013) or an increase in transmembrane pathway (Morillon and Chrispeels 2001; Martre et al. 2002).

The drought-induced phytohormone abscisic acid (ABA) can affect transmembrane transport via the levels of expression, phosphorylation, and/or degradation of AQPs (reviewed by Shivaraj et al. 2021). ABA has been shown to reduce the membrane osmotic water permeability (P_f) of BSC via AQPs, to have no effect on the P_f of mesophyll protoplasts (Shatil-Cohen et al. 2011) and to link the transmembrane water pathway and regulation of K_{leaf} via nonstomatal mechanisms (Pantin et al. 2013; Coupel-Ledru et al. 2017). Conversely, ABA fed through the roots was reported to increase the P_f of wild-type (WT) mesophyll protoplasts after 24 h and that of *aba1* (mutants with impaired ABA synthesis) protoplasts after 3 h (Morillon and Chrispeels 2001).

Focusing on the symplastic pathway, only a few works have studied the effects of ABA and abiotic stress on plasmodesmata. Those works have reported inconsistent results regarding increased (Erwee and Goodwin 1984; Schulz 1995) or reduced (Cui and Lee 2016; Kitagawa et al. 2019) permeability of the plasmodesmata. We hypothesized that ABA might have a direct effect on the symplastic water pathway, in addition to its effect on the transmembrane water pathway.

In addition to its widely studied role as a stress hormone, low basal levels of ABA have recently been shown to play a major role in physiological and developmental mechanisms related to plant water status (reviewed by Yoshida et al. 2019), for example, setting the steady-state stomatal aperture (Merilo et al. 2018; Yaaran et al. 2019). However, to the best of our knowledge, the effects of basal ABA on K_{leaf} and, particularly, on K_{ox} have not yet been investigated.

The general goal of the current study was to improve our understanding of the leaf hydraulic maze, particularly along the BSC and MC continuum. We hypothesized that K_{ox} is dynamically regulated by the BSC and MC symplastic, transmembrane and apoplastic pathways in a manner that is controlled by ABA, from the low basal ABA levels observed under optimal growth conditions to the higher ABA levels that are associated with drought. This study investigates and compares the osmotic water permeabilities of spongy mesophyll, palisade mesophyll, and BSC in the context of the regulation of leaf water balance under optimal and high-ABA conditions. To test this hypothesis, we constructed tissue-specific ABA-insensitive plants by expressing the negative semidominant *abi1-1* mutant gene under a tissue-specific promoter, to generate mesophyll ABA-insensitive (MCabi) plants (plants with ABA-insensitive MC) (Negin et al. 2019) and bundle sheath ABA-insensitive (BSabi) plants (plants with ABA-insensitive BSC), both of which maintained a WT-like stomatal response to ABA. In this work, we address the effects of tissue-specific insensitivity to ABA from the cellular level through whole-plant transpiration rates.

Results

Characterization of the BSabi and MCabi phenotypes

To better understand the effects of ABA on leaf hydraulics, we generated tissue-specific ABA-insensitive lines. We expressed the dominant *abi1-1* (ABA-insensitive) mutation under the FBPase promoter (for expression in green tissues, but not in guard cells), to create plants that had suppressed ABA signaling in their MC and BSC (i.e. MCabi plants), or under the SCR promoter (for expression in BSC, but not in MC), to create *Arabidopsis* (*Arabidopsis thaliana*) plants with

suppressed ABA signaling in their BSC (i.e. BSabi plants; see Materials and methods). The strongest effect of *abi1-1* is expected at the site where it is expressed; nevertheless, we cannot exclude its potential for cell-to-cell movement. Three independent lines were selected for each mutation (MCabi: 1, 2, and 7; BSabi: 12, 14, and 99).

The MCabi plants were broadly characterized and validated (Negin et al. 2019), and the same validation was performed for the BSabi plants (Supplemental Fig. S1, A to C). MCabi and BSabi lines exhibited different phenotypes. MCabi's leaves were larger and thicker than those of the WT, while BSabi had smaller leaves (Fig. 1, A, B, and F). BSabi maintained the same proportion of palisade to spongy MC as the WT; whereas MCabi had more space occupied by palisade MC (Fig. 1F). Despite the changes in leaf size, the vein densities of BSabi and MCabi remained the same as that of the WT (Fig. 1C), with BSabi differing from the WT in its narrower veins but only MCabi differing from WT in its increased xylem to total vein ratio (Fig. 1G). Moreover, the steady-state stomatal aperture (Fig. 1D) and stomatal index (Fig. 1E) of MCabi were greater than those of the WT and BSabi. Both MCabi and BSabi plants had a WT-like stomatal response to ABA (Negin et al. 2019; Supplemental Fig. S1C), and their average foliar ABA levels were similar to those of the WT (Supplemental Fig. S2, A and B; 1 of the 3 BSabi lines had ABA levels that were higher than those of the WT).

Gas exchange and leaf hydraulics

To assess the relative contributions of the MC and BSC to the overall K_{leaf}, we performed gas-exchange measurements and then measured Ψ_{leaf} using a pressure chamber. The experiment was first done for each transgene separately (Supplemental Fig. S3). All 3 independent lines were found to be similar to one another, and the experiment was then repeated with MCabi and BSabi together, so that they could be compared at the same time under the same conditions (Fig. 2). Under optimal conditions, BSabi and MCabi had similar levels of transpiration (E), which were higher than that of the WT. Yet, despite that higher E, both types of transgenic plants maintained Ψ_{leaf} that was similar to that of the WT, resulting in higher K_{leaf} than the WT (Fig. 2, A to C). BSabi and MCabi exhibited higher stomatal conductance (g_s) accompanied by only slightly higher net carbon assimilation rate (A_N), resulting in lower intrinsic water-use efficiency (iWUE; Fig. 2, D to F). Following ABA treatment, all lines exhibited reduced E, g_s and, surprisingly, K_{leaf} (Fig. 2, A and C). MCabi and BSabi maintained an unaltered stomatal ABA response (Supplemental Fig. S1C; Negin et al. 2019) and, therefore, reduced their g_s and E in response to ABA (Fig. 2, A and D). However, while ABA reduced the Ψ_{leaf} of the WT, the Ψ_{leaf} levels of MCabi and BSabi remained unchanged (Fig. 2B). Consequently, the K_{leaf} reduction observed in MCabi and BSabi was mainly related to their reduced transpiration (Fig. 2, A to C). Overall, this resulted in higher iWUE for the WT, as compared to the 2 sets of transgenic lines, even following ABA treatment (Fig. 2F).

Although MCabi plants had a higher stomatal index and larger stomatal apertures than the BSabi plants (Fig. 1, D and E), they had similar E and g_s (Fig. 2, A and D). E was measured in an enclosed gas-exchange chamber, in which it was difficult to maintain a constant vapor pressure deficit (VPD) at high levels of E (Supplemental Fig. S4). To overcome this challenge, we measured whole-plant transpiration in an open space, under natural conditions, using a gravimetric system in which all plants were simultaneously exposed to the same VPD (Fig. 3, A to D). We found that the MCabi plants had the highest transpiration rate (Fig. 3E). This trend was maintained throughout the whole growing period (40 d; Supplemental Fig. S5, A to C). When transpiration was normalized to plant weight, MCabi plants still had the highest E, with BSabi plants exhibiting intermediate level E and WT plants exhibiting the lowest E (Fig. 3F). The highest E in MCabi suggests that the mesophyll participates in the regulation of E, although the exact mechanism remains unclear.

Differences between the palisade and spongy MC: P_f and ABA response

To study the mesophyll's contribution to E and K_{leaf}, in general, and the specific contributions of palisade and spongy MC, we used reporter lines with palisade (*IQD22pro::GUS-mCit*) and lower spongy (*CORI3::GUS-mCit*) tissue-specific labeling with the fluorescent protein mCit (Procko et al. 2022) and examined the P_f of each type of cell. The 2 reporter lines revealed largely restricted labeling; we did not find any apparent labeling on any other leaf tissue, including the bundle sheath and guard cells (Fig. 4, A and B). Spongy mesophyll protoplasts exhibited higher P_f under control conditions (Fig. 4C) and were smaller than the palisade protoplasts (Fig. 4D). The P_f values of both types of protoplasts showed a tailed distribution, with most of the protoplasts having low P_f values. Yet, even when we considered only 90% of the population, to exclude the "tails" of the populations, the P_f of the spongy mesophyll protoplasts remained almost double that of the palisade protoplasts. Moreover, more spongy mesophyll protoplasts had extreme P_f values of over 60 $\mu m\ s^{-1}$. In response to ABA, the higher P_f of the spongy mesophyll protoplasts was reduced by roughly 60% ($19.2 \pm 0.7\ \mu m\ s^{-1}$ to $7.2 \pm 1.8\ \mu m\ s^{-1}$, respectively); whereas the average P_f of the palisade protoplasts did not change (Fig. 4E).

To examine the effect of ABA insensitivity on MC, we fluorescence-labeled palisade and spongy mesophyll protoplasts of the MCabi#2 line. Surprisingly, we found that ABA insensitivity in the spongy mesophyll reduced the P_f of spongy mesophyll protoplasts, but did not affect the P_f of palisade protoplasts (Fig. 5A). Moreover, MCabi spongy protoplasts maintained their low P_f at increasing concentrations of ABA and remained insensitive to ABA even when they were exposed to 50 μM ABA (Fig. 5C).

We also used fluorescence-labeled ABA-insensitive BSCs of the BSabi#14 line to investigate the effect of ABA insensitivity

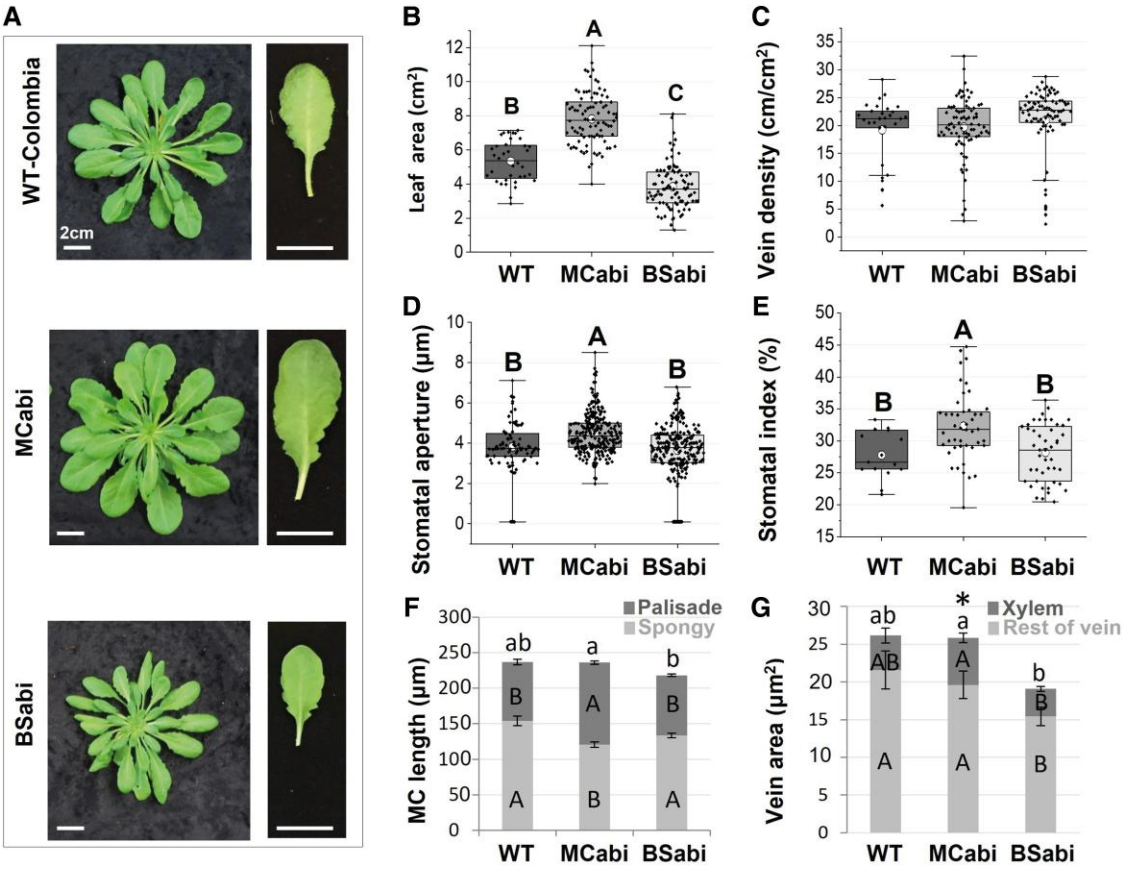

Figure 1. Mcabi and BSabi phenotypes. Morphological characteristics of 7- to 8-wk-old MCabi and BSabi plants grown under short-day conditions, including **A)** representative images of the rosettes and fully expanded leaves of each line (bar = 2 cm), **B)** leaf area, **C)** vein density, **D)** stomatal aperture, **E)** stomatal index, and **F)** total leaf thickness divided by the widths occupied by palisade (dark gray) and spongy (light gray) mesophyll. Capital letters refers to significant differences between each mesophyll layer and lower-case letters refer to significant differences in total leaf thickness (Tukey's test, $P < 0.05$). **G)** Vein area divided into the area occupied by the xylem (dark gray) and the rest of the vein area (light gray). An asterisk indicates a significantly higher ratio of xylem to total vein area, capital letters refer to significant differences between the xylem and the rest of the vein area, and lower-case letters refer to significant differences in total vein area (Tukey's test, $P < 0.05$). **B** to **E)** The box height shows 25% to 75% of the data range, the symbols indicate the individual data values, the solid line indicates the median, o indicates the mean and the whiskers delimit ±3 times the interquartile range. **F** to **G)** Data are means ± SE. **B)** $n = 36$ for WT and 90 for MCabi and BSabi, 5 leaves from 6 plants for each transgenic line. **C)** $n = 10$ leaves for WT and 28 to 30 for MCabi and BSabi, 9 to 10 leaves from each transgenic line, an average of 2 to 3 patches of ~1 cm^2 per leaf. **D)** $n = 80$ stomata for WT and >245 for MCabi and BSabi, ~ 80 stomata from each transgenic line, and 20 stomata from 4 leaves for each. **E)** $n = 80$ stomata for WT and >245 for MCabi and BSabi, ~ 80 stomata from each transgenic line, and 20 stomata from 4 different leaves for each. **F** and **G)** $n = 5$ leaves for WT and 15 for MCabi and BSabi, 5 leaves from each transgenic line, and an average of 3 cross sections per leaf.

in the bundle sheath and found that insensitivity increased the P_f of the bundle sheath protoplasts (Fig. 5B). BSabi#14 bundle sheath protoplasts also preserved their ABA insensitivity, and their P_f did not change in response to increasing ABA concentration (Fig. 5D).

Taken together, both basal and higher levels of ABA appear to affect the movement of water across spongy MC and BS membranes, affecting the transmembrane water pathway. Next, we were interested in exploring the effects of ABA on the movement of water through the symplastic pathway.

Effects of ABA on the symplastic water pathway

To evaluate the relative contribution of the symplastic water pathway to the total K_{leaf}, we measured the K_{leaf} of known mutants with severely altered plasmodesmatal permeability: *CalS 8-1*, whose plasmodesmatal permeability is ~35% higher than that of the WT (Cui and Lee 2016), and *AtBG_ppap*, whose plasmodesmatal permeability is ~45% lower than that of the WT (Zavaliev et al. 2013). The K_{leaf} values of both mutants were similar to that of the WT (Fig. 6A) and their g_s, E, and Ψ_{leaf} were similar as well (Supplemental Fig. S6). Next, we used the drop-and-see (DANS) assay (Cui and Lee 2016) to measure the relative plasmodesmatal permeability of MCabi and BSabi under control conditions and in response to ABA treatment. In principle, the cell-to-cell spread of a fluorescent dye can be used to measure the permeability of the plasmodesmata (this spread can be seen in the top of Fig. 6B, marked by yellow circles. For

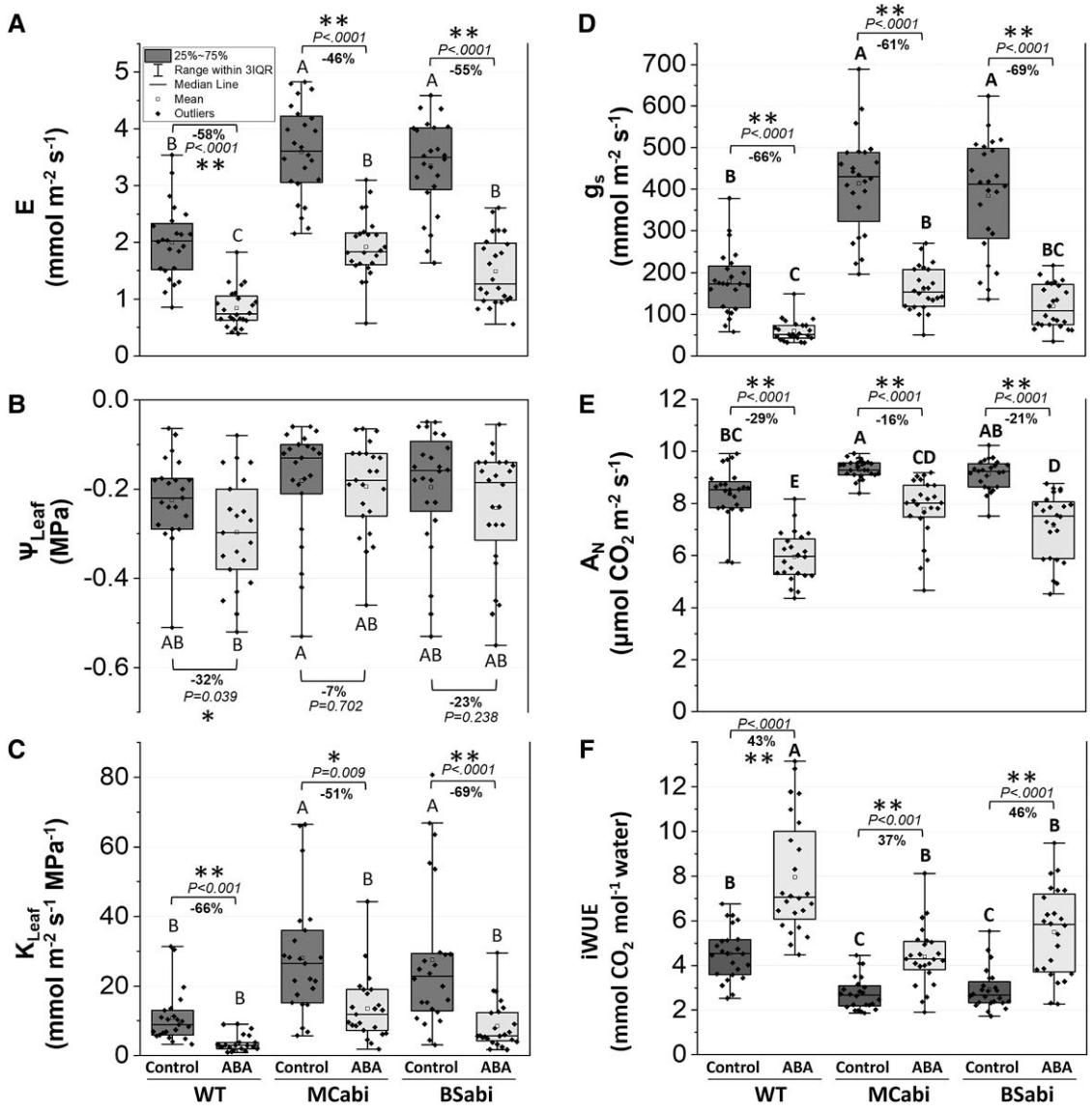

Figure 2. Gas exchange of WT, MCabi and BSabi leaves under nonstressed conditions in the presence of xylem-fed ABA. Leaves of 6- to 8-wk-old plants were cut before dawn and petiole-fed AXS (dark gray) or AXS +10 μM ABA (light gray). After 1 to 4 h, the **A**) whole-leaf transpiration rate **E)** and **B**) leaf water potential, Ψ_{leaf}, were measured, enabling the calculation of **C)** leaf hydraulic conductance, K_{leaf}, for each individual leaf. In addition, the **D**) stomatal conductance, g_s, and **E)** net carbon assimilation rate, A_N, were measured, enabling the calculation of **F**) iWUE for those same leaves. The percentage change following the ABA treatment is indicated as well. Data were analyzed using 2-way ANOVA (all model effects and interactions are presented in Supplemental Table S1.) Different letters indicate significant differences according to Tukey's HSD test ($P < 0.05$); *P*-values of the effect of each treatment on each genotype according to *t*-tests are also indicated. The box height shows 25% to 75% of the data range, the symbols indicate individual data values, the solid line indicates the median, o indicates the mean, and the whiskers delimit ±3 times the interquartile range of at least 3 independent experiments. $n = 21$ leaves for WT and 23 to 24 leaves for MCabi and BSabi and 7 to 8 leaves from each transgenic line.

more detailed information, see Material and methods). Under control conditions, the relative plasmodesmatal permeability of the MCabi plants was highest, that of the BSabi was intermediate, and the WT had the lowest relative plasmodesmatal permeability (Fig. 6B). This ranking corresponds to the ranking of those lines' E under greenhouse conditions (Fig. 3F).

Following ABA treatment, only WT leaves exhibited significantly increased relative plasmodesmatal permeability (Figs. 5B and S7A for detailed information for each line). Changes in plasmodesmatal permeability can be attributed to the accumulation of callose (a β-1,3-glucan) in the plasmodesmata (Amsbury et al. 2017). Nevertheless, there were no detected changes in the callose levels in either of the lines in any of the treatments in our experiment (Supplemental Fig. S7B). Validation of proper callose staining was done on leaves that had been pretreated with flagellin, whose reduced relative plasmodesmatal permeability was accompanied by increased callose deposition, as expected (Supplemental Fig. S8).

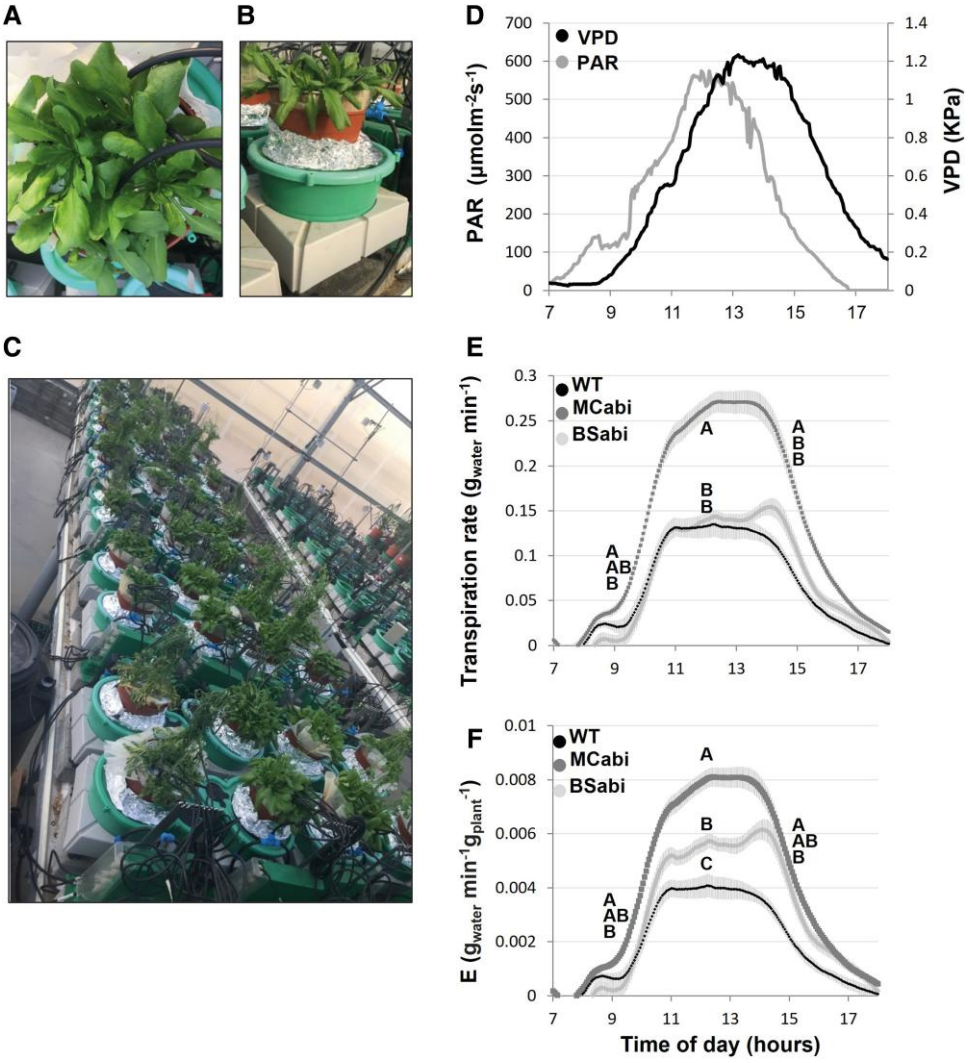

Figure 3. Continuous measurements of whole plants under greenhouse conditions. **A)** Top view and **B)** side view of pots with 8-wk-old WT *Arabidopsis* plants, 4 plants per pot. All pots were randomized and measured simultaneously on **C)** a lysimeter system located in a greenhouse under semi-controlled conditions. The plants were exposed to **D)** ambient VPD and photosynthetic photon flux density (PPFD) of the photosynthetically active radiation (PAR) conditions as shown here for 1 representative day, the 11th day after the pots were loaded onto the lysimeters. **E)** Whole-plant continuous transpiration rates (gram of water per minute) of WT (black), MCabi (dark gray), and BSabi (light gray). **F)** Transpiration (gram of water per minute per gram plant) of the different lines normalized to plant weight. Data are means + SE ($n = 5$ pots for WT and 18 to 19 for MCabi and BSabi, 6 to 7 pots from each transgenic line, 4 plants in each pot). Letters indicate significant differences at 09:00, 12:00, and 15:00, according to Tukey's test ($P < 0.05$).

Discussion

BSC and MC control K_{leaf} and transpiration via ABA regulation

The working hypothesis in this study was that K_{ox} is controlled by a series of living cells, including BSC and MC. Our results suggest that the P_f levels of BS and spongy MC are a target of basal and higher ABA levels, while the way that they regulate K_{leaf} may not be straightforward. The increased E and K_{leaf} observed among both BSabi and MCabi under optimal conditions implies that in the WT, E and K_{leaf} are limited by a nonstomatal mechanism, most likely involving the effect of basal ABA on physiological and developmental regulation.

Recently, it has been suggested that the basal levels of ABA expressed under nonstress conditions limit the steady-state stomatal aperture (Merilo et al. 2018; Yaaran et al. 2019). Our finding that BSC insensitivity to ABA results in increased P_f (Fig. 5B) and elevated K_{leaf} in BSabi under control conditions (Fig. 2C) suggests ABA may play a similar role in BSC-specific regulation. This dual restricting role (in the guard cells and in the BSC) of basal ABA may serve to preserve leaf water balance by balancing leaf water influx (via bundle sheath) and efflux (via guard cells) to sustain overall water flow and content. We further suggest that this role of basal ABA is augmented by its activity under stress conditions when high ABA levels reduce both stomatal apertures

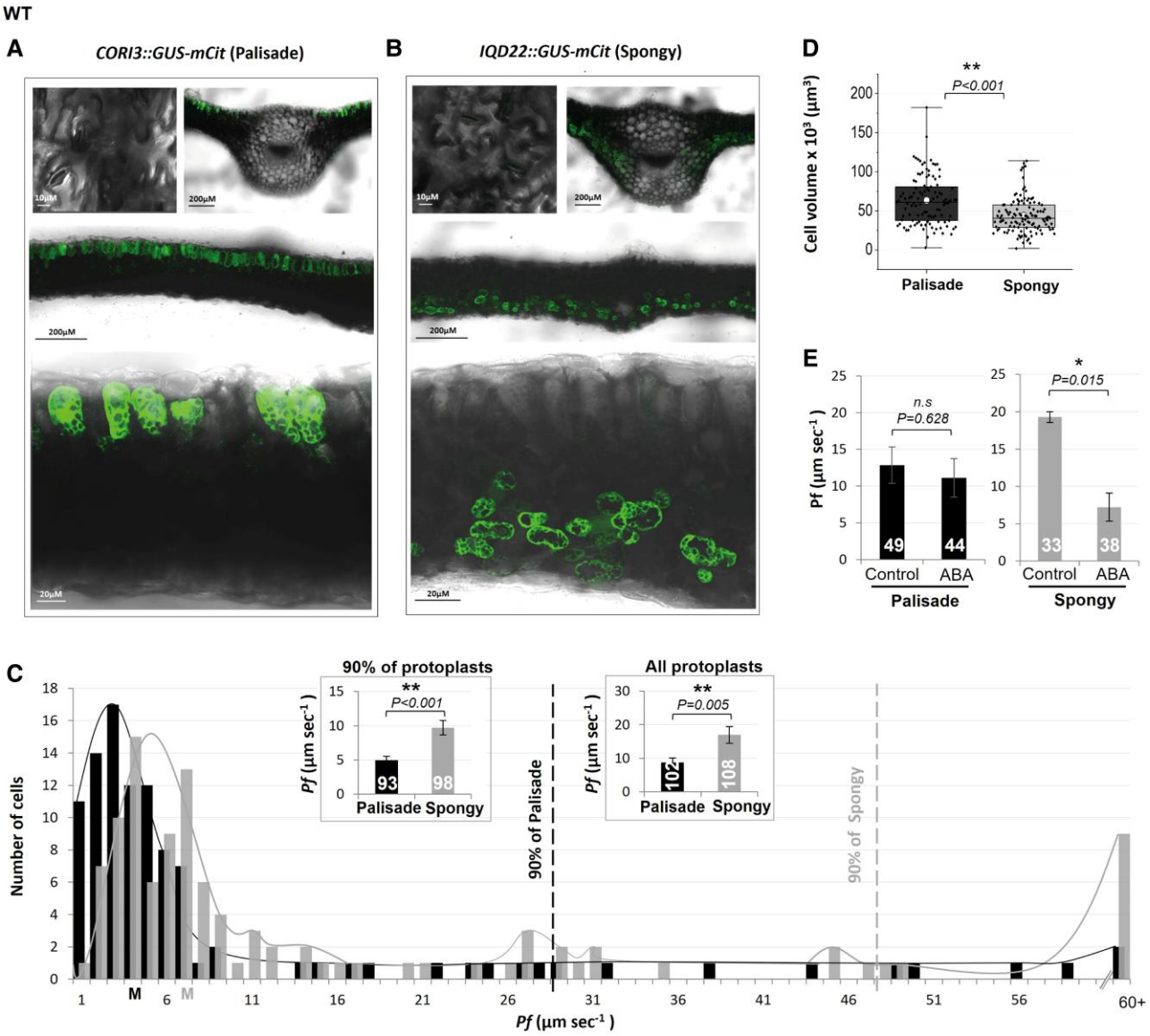

Figure 4. Osmotic water permeability coefficients (P_f) of palisade mesophyll and spongy mesophyll protoplasts. **A)** Fluorescent images of the stomata and cross sections of *Arabidopsis* leaves expressing a GUS-mCitrine reporter protein under a palisade-specific promoter (IQD22) or **B)** a spongy MC-specific promoter (CORI3); bar sizes are shown in the images. **C)** P_f distributions of WT palisade (black) and spongy (gray) MC protoplasts generated from IQD22::GUS-mCit and CORI3::GUS-mCit reporter lines, respectively. Dashed lines define the "tail" of the top 10% outstanding P_f values of the "high-P_f" for both types of protoplasts (>28 μm s^{-1} for palisade and >47 μm s^{-1} for spongy). Means ± SE of 90% of the populations is also shown. M, median. **D)** Volumes of palisade (gray) and spongy (black) protoplasts. The box height shows 25% to 75% of the data range, the symbols indicate individual data values, the solid line indicates the median, o indicates the mean, and the whiskers delimit ±3 times the interquartile range. **E)** P_f response to pretreatment with 1 μM ABA (1 to 4 h). Comparison between the 2 populations is according to Student's *t*-test **C** to **E**), 1asterisk indicates a *P*-value less than 0.05 and 2 asterisks indicate a *P*-value less than 0.01. The *P*-values are presented in the figure. Protoplast numbers are shown in each bar.

and K_{leaf}. It is interesting to note that similarities between the regulation mechanisms of guard cells and BSC have also been reported in the context of blue light, which initiates stomatal opening while increasing bundle sheath P_f (Iino et al. 1985; Zait et al. 2017; Torne et al. 2021; Grunwald et al. 2022). Such a role for the bundle sheath also reinforces its importance as a leaf hydraulic checkpoint (Ache et al. 2010; Griffiths et al. 2013; Caringella et al. 2015).

Nevertheless, higher hydraulic conductance of BSabi and MCabi comes with penalty of lower iWUE due to a major increase in E as compared to WT (168% to 180% Fig. 2A and 68% to 80% Fig. 3F), accompanied by a minor increase in the carbon assimilation rate, A_N (~10%, Fig. 2E). As E increases linearly with stomatal aperture, while A_N has a maximal saturation point, the optimized WUE falls within the nonmaximal gas-exchange range (Yoo et al. 2009),

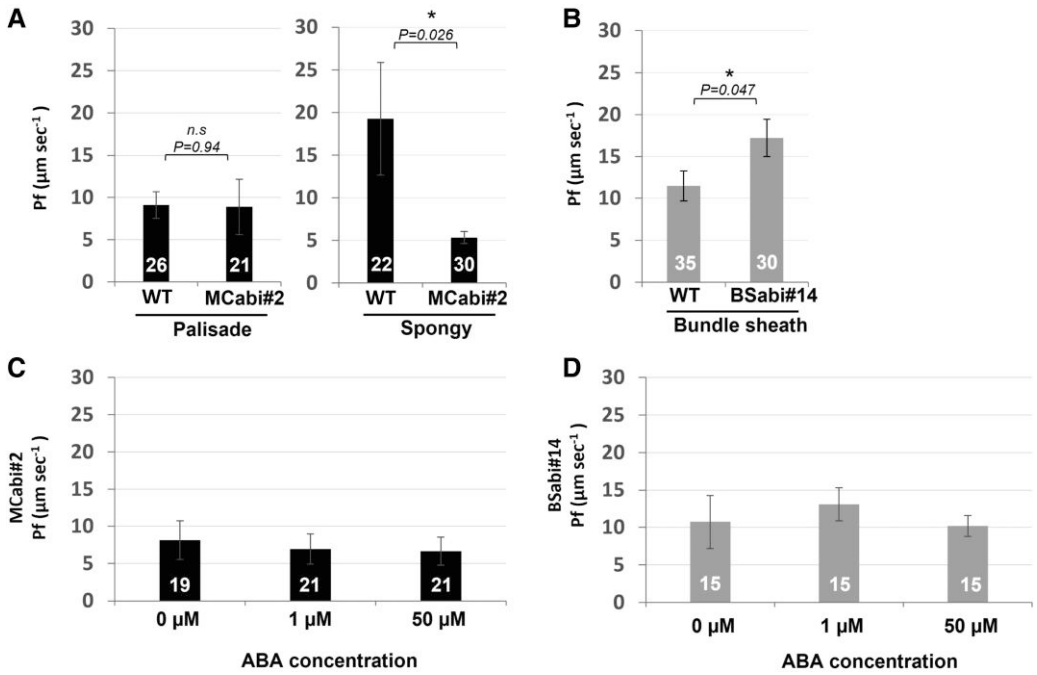

Figure 5. Osmotic water permeability coefficients (P_f) of MCabi and BSabi protoplasts in response to increasing ABA levels. **A)** P_f levels of palisade and spongy mesophyll protoplasts of WT and MCabi#2 (ABA-insensitive) carrying the palisade (*IQD22::GUS-mCit*) and spongy (*CORI3::GUS-mCit*) markers under nonstressed conditions. **B)** P_f levels of bundle sheath protoplasts of WT and BSabi#14 (ABA-insensitive) carrying the BSC marker SCR::GFP under nonstressed conditions. **C)** P_f responses of spongy mesophyll of MCabi#2 and **(D)** of the bundle sheath of BSabi#14 to pretreatment with increasing levels of ABA: 0, 1, and 50 μM ABA (1 to 4 h). Data are means ± SE from at least 4 independent experiments. For **A** and **B**, an asterisk indicates a *P*-value of less than 0.05, according to Student's *t*-test. The *P*-values are presented in the figure. For **C** and **D)**, there were no significant differences between the ABA concentrations, according to Tukey's HSD test. Protoplast numbers are presented inside each bar.

supporting that the photosynthetic system is saturated at high K_{leaf} (Brodribb et al. 2005). Therefore, nonmaximal hydraulic conductance and E under optimal growth conditions may have a selective advantage at the evolutionary time scale, preventing excessive water loss that would provide only minimal gains in productivity.

Under ABA treatment, both BSabi and MCabi maintained high, unaltered Ψ_{leaf} (Fig. 2B), indicating that BSC and MC contribute to Ψ_{leaf} regulation. Still, these plants exhibited strong reductions in E (46% to 55%), resulting in K_{leaf} reduction. This discrepancy, however, may highlight the limitations of our current methods in independently assessing leaf hydraulic conductance (calculated from 2 different measurements, E and Ψ_{leaf}), suggesting that complex, interrelated factors within the leaf system, potentially masked by strong stomatal responses, may be at play. Furthermore, the examination of the ABA effect on leaf internal tissues via K_{leaf} is challenging due to ABA's dual influence on stomata (Pantin et al. 2013). As such, the current methods for calculating K_{leaf} might obscure the ABA response of BSC and MC, which is indicated by their consistent Ψ_{leaf}.

Palisade and spongy MC differ in their hydraulic properties

To better understand MC's contribution to leaf hydraulics, we examined palisade and spongy MC which differ in both their structure and their hydraulic properties (Fig. 4; Canny 2012; Buckley et al. 2015; Álvarez-Arenas et al. 2018; Muries et al. 2019) separately. Based on our findings, the P_f of the spongy MC under nonstressed conditions was almost twice that of the palisade MC (Fig. 4, C and E). The spongy mesophyll's vast exposure to the leaf's internal air spaces together with its high P_f may explain those cells' rapid loss of water and shrinkage upon high VPD (Canny 2012) or dehydration (Muries et al. 2019). This is an intriguing point, which may suggest that spongy MC act as hydraulic sensor in the following way: high P_f enables the rapid loss of water content, resulting in decreased cell volume, which lessens cell wall and plasma membrane interactions, to induce ABA production (Bacete et al. 2022). In this way, a physical change, such as high VPD, can be translated into a physiological response of stomatal closure (Mott and Parkhurst 1991). Surprisingly, MCabi exhibited high K_{leaf} (Fig. 2C) despite its spongy MC's low P_f, suggesting that its high K_{leaf} is mainly supported by a bundle sheath that is insensitive to ABA and/or apoplastic flow. The observation that changes in P_f do not align with K_{leaf} measurements is surprising and important. Nevertheless, it may underscore the limitations in our current ability to assess hydraulic conductance independently of the stomata, in the context of the entire leaf, rather than pointing simple lack of association between the two. The low P_f of MCabi spongy MCs could result

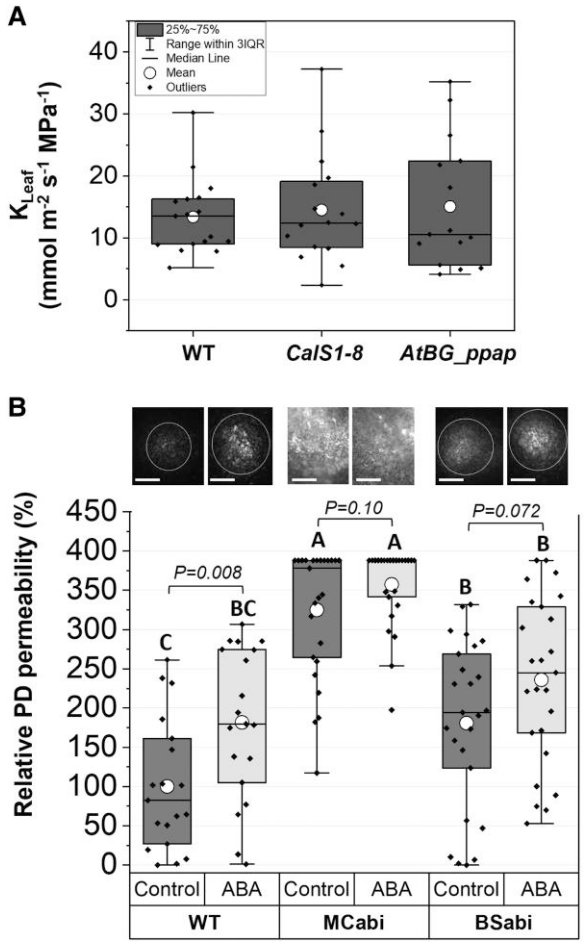

Figure 6. Effects of ABA on the symplastic and apoplastic pathways. **A)** leaf hydraulic conductance (K_{leaf}) of mutants with impaired plasmodesmatal (PD) permeability. **B)** DANS assays revealed the cell-to-cell spread of fluorescence in WT, MCabi, and BSabi plants that were petiole-fed AXS (dark gray) or AXS +10 μM ABA (light gray). Top of **B)**: Yellow circles show the cell-to-cell spread of the fluorescent dye (bar = 20 μm). The box height shows 25% to 75% of the data range, the symbols indicate individual data values, the solid line indicates the median, o indicates the mean, and the whiskers delimit ±3 times the interquartile range of at least 3 independent experiments. For **A)**, data were analyzed using 1-way ANOVA. For **B)**, data were analyzed using 2-way ANOVA (all model effects and interactions are presented in Supplemental Table S1.) Different letters indicate significant differences according to Tukey's HSD test ($P < 0.05$); *P*-values of the effect of each treatment on each genotype according to *t*-tests are also indicated. **A)** $n = 15$ to 17 leaves; **B)** $n = 19$ for WT and 24 to 25 for MCabi and BSabi, 8 to 9 leaves from each transgenic line.

from hydraulic feedback from high transpiration rates, as suggested by Morillon and Chrispeels (2001), negative feedback from increased water supply in neighboring BSCs reducing P_f in spongy MCs, or additional, as yet, unknown reasons.

In response to higher ABA levels, the WT spongy MC reduced its P_f to avoid further water loss, while the palisade P_f remained unchanged (Fig. 4E), highlighting tissue-specific ABA regulation. Palisade MC's lack of response to ABA supports that these cells play a static hydraulic role (Zwieniecki et al. 2007), in which they serve as a water buffer to maintain leaf water balance (Nardini et al. 2010; Rockwell et al. 2014). The combination of palisade mesophyll with static hydraulic properties and the lack of any direct effect of ABA on photosynthesis (Negin et al. 2019) can be an advantage for continued photosynthesis (Tholen et al. 2012; Buckley 2015) and position ABA as, primarily, a water balance regulator (from BSC to guard cells).

The role of plasmodesmata in the symplastic water pathway and K_{ox}

To evaluate the roles of plasmodesmata and the symplastic water pathway in K_{leaf}, we used impaired plasmodesmata permeability mutants (*cals8-1*, Cui and Lee 2016; and *AtBG_ppap*, Zavaliev et al. 2013). Both exhibited WT-like K_{leaf} (Fig. 5A), indicating that the symplastic pathway has a negligible influence on K_{leaf}. Moreover, the fact that ABA increased the WT's symplastic permeability (Fig. 5B), alongside its reduction of K_{leaf}, supports this idea. As high ABA levels reduce P_f while increasing plasmodesmatal permeability, the symplastic water flow may provide better cell-to-cell conductivity and turgor sharing to help maintain uniform water potential across the tissue. Additionally, it may act as a rapid facilitator of the stress signal by distributing the ABA among the cells.

The greater symplastic conductivity of BSabi and the even greater symplastic conductivity of MCabi under control conditions are, therefore, surprising (Fig. 6B). Here, we present 3 possible explanations: (i) Altered development. During sink-to-source transition, the leaves' plasmodesmata are dramatically reduced (Roberts et al. 2001). Therefore, impaired maturation may sustain a higher number of plasmodesmata. Interestingly, *abi1-1* hybrid aspen trees fail to block their plasmodesmata as they enter dormancy (Tylewicz et al. 2018). (ii) Impaired hormonal cross talk with salicylic acid which reduces the permeability of plasmodesmata (Wang et al. 2013; Cui and Lee 2016). ABI1 binds directly to salicylic acid and impairs that cross talk (Manohar et al. 2017). The relatively low levels of salicylic acid observed in MCabi and BSabi (Supplemental Fig. S2C) support such altered cross talk, which may affect plasmodesmata permeability. (iii) *abi1-1* protein signaling function. While *abi1-1* mutants lack phosphatase activity, the protein itself may have a signaling function (Gosti et al. 1999). If plasmodesmatal permeability involves such an ABA-signaling pathway, it may be boosted in the transgenic plants due to the high abundance of *abi1-1* in the specific tissue.

A suggested model for the role of ABA in the regulation of K_{leaf}

Integrating our results, we suggest the following hypothetical model of radial water movement within the out-of-xylem leaf tissues (Fig. 7). Under optimal conditions, water enters the leaf through the BSC, which selectively regulate

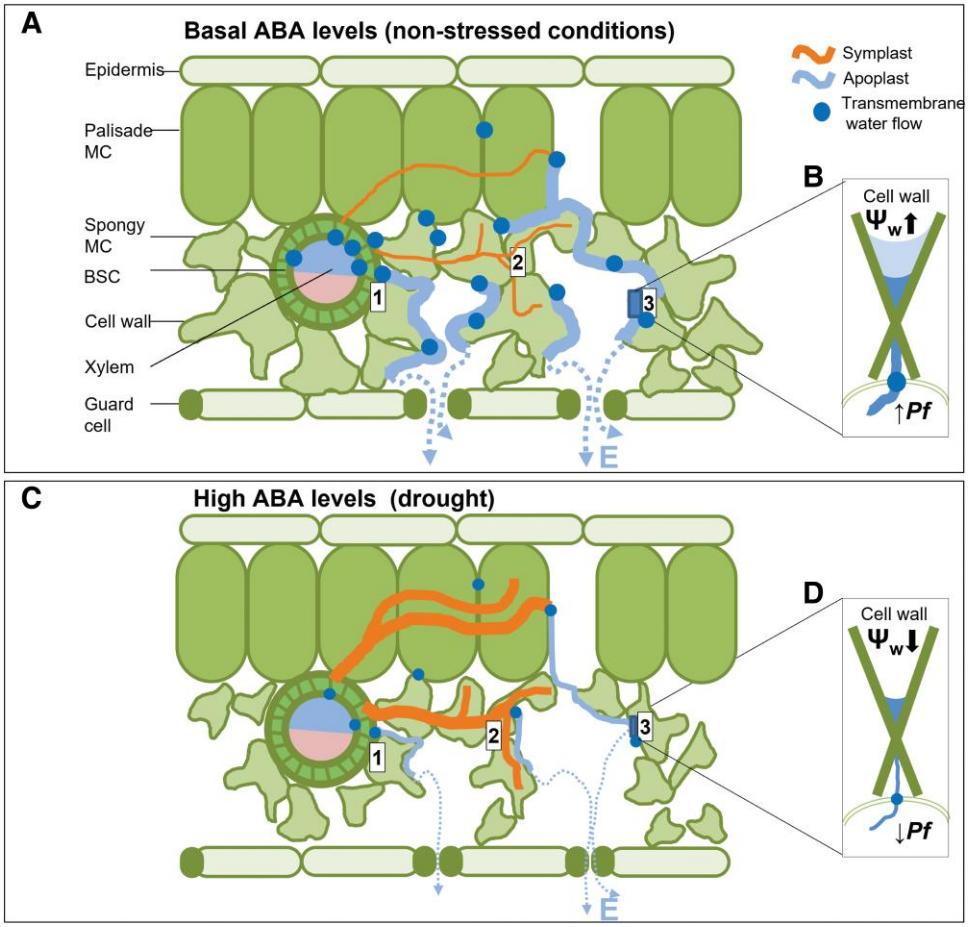

Figure 7. A suggested model for ABA's regulation of leaf hydraulic conductance. **A)** Under optimal conditions, water flows across the BSC via the transmembrane water pathway, probably through AQPs (blue dots; Control Point 1) and proceeds toward the MC. In the mesophyll, water may flow in parallel pathways and move between them. The apoplastic (light blue line) and transmembrane pathways are dominant, while the contribution of the symplastic path (dark red line) is relatively small (Control Point 2). **B)** The transmembrane water permeability (P_f) of the spongy MC can facilitate the export of water from cells, contributing to transmembrane water flow or directing water toward the cell wall to support apoplastic water flow (Control Point 3) and transpiration (E, dashed blue line). Note that under optimal conditions, most water flows through the spongy MC, preserving leaf water status (e.g. high leaf water potential, Ψ_{leaf}, and turgor). **C)** High levels of ABA reduce the P_f of the BSC (blue dot, Control Point 1. Shatil-Cohen et al. 2011). In the immediate term, less water enters the leaf, while the amount of water leaving through the stomata remains high, which causes the spongy MC to shrink (Canny 2012) due to their high initial P_f, amplifying the stress signal and initiating ABA production (Bactete et al. 2022). Higher ABA then decreases the spongy MC's P_f and **(D)** decreases the transmembrane water flow and apoplast wetting (Control Points 2 and 3). Diminished flow over the transmembrane and apoplastic water pathways (blue dots and light blue line, respectively) keeps water inside the cells, while ABA increases the amount of water transported via the symplastic pathway (red line; Control Point 2). The effects of all the above combined with the direct effect of ABA on stomata result in reduced leaf hydraulic conductance, K_{leaf}, and E (dashed blue line) as the leaf's water status deteriorates (e.g. reduced Ψ_{leaf} and turgor).

transmembrane radial water flux (Fig. 7A, Control Point 1; Leegood 2008; Galvez-Valdivieso et al. 2009; Shapira et al. 2009; Ache et al. 2010; Shatil-Cohen et al. 2011; Prado and Maurel 2013; Grunwald et al. 2021) based on the osmotic water permeability of their membranes, regulated by basal ABA (Fig. 5B). Then, water proceeds toward and within the MC. The transmembrane pathway (Cochard et al. 2007; Kim and Steudle 2007), which mostly follows via the spongy MC (Fig. 4C; Buckley et al. 2015; Buckley 2015; Xiong and Nadal 2020), and the apoplastic pathway (Sack and Holbrook 2006; Voicu et al. 2009; Buckley 2015) govern K_{leaf} under optimal conditions, while the contribution of the symplastic pathway is negligible (Figs. 6 and 7A, Control Point 2).

The high P_f of the spongy MC may have 2 advantages, allowing the spongy mesophyll to serve as an interchange point between the parallel water pathways and as a hydraulic sensor. Water crossing a cell membrane may continue toward the next cell in the transmembrane pathway or remain in the apoplast, wetting the cell wall to support the apoplastic water pathway (Maurel 1997; Steudle and Peterson 1998; Fig. 6A, Control Point 3). As a hydraulic sensor, the spongy mesophyll's large surface area combined with its high P_f results in rapid water loss when there is an imbalance between

water supply and demand, quickly reducing the cell's volume, offering a conceivable mechanism to capture changes in the rate of water loss from the leaf. The simultaneous limitation of K_{leaf} and stomatal aperture by basal ABA levels maintains the balanced leaf water status that is mirrored in the high Ψ_{leaf} and turgor (Fig. 7A).

In the presence of a high level of ABA, xylem ABA reduces the BSC's P_f (Shatil-Cohen et al. 2011; Fig. 7C, Control Point 1), which limits water flow into the leaf. In the immediate term, the stomatal efflux remains , and the spongy MCs' high initial P_f (Fig. 4C) results in their rapid water loss, shrinkage (Canny et al. 2012; Muries et al. 2019), and ABA production (McAdam and Brodribb 2016; Sussmilch et al. 2017; Sack et al. 2018; Bacete et al. 2022; Fig. 7, A and B). When they sense ABA, the spongy MCs decrease their P_f (Figs. 4E and 7C, Control Point 2; Fig. 7B), resulting in the retention of water within the mesophyll and reducing the flow over the transmembrane water pathway, cell wall wetting and, subsequently, the apoplastic flow (Fig. 7, C and D, Control Point 3). As a result of all the above and the direct effect of ABA on stomata, K_{leaf} and g_s decrease, while the leaf water status deteriorates (e.g. decreased turgor and Ψ_{leaf}). Simultaneously, the high ABA levels increase the symplastic permeability (Figs. 6B and 7C, Control Point 2). This may facilitate the cooperation of MC and solute transport when E levels are low (Morillon and Chrispeels 2001) and may enhance the symplastic passage of ABA through the leaf and toward the guard cells.

This study highlights the differential effects of ABA on BSCs, spongy and palisade MCs, as well as the effects of those tissues on K_{leaf}. Our efforts to untangle the effects of ABA on leaf hydraulics have revealed that a series of living cells, which are differentially affected by ABA, take part in determining leaf water balance under optimal and high-ABA conditions.

Materials and methods

Plant material and growing conditions

All of the *Arabidopsis* (*A. thaliana*) plants used in this study were of the Colombia (col) ecotype (WT). In addition to WT plants, we also used transgenic FBPase::*abi1-1* (MCabi; Negin et al. 2019) and SCR::*abi1-1* (BSabi) plants. *CalS8-1* (037603C) was generously provided by Jung-Youn Lee, and *AtBG_ppap* (SAIL_115_G04) was ordered from SALK (Loughborough, UK). PCR was used to confirm the homozygosity of both of those lines. *CORI3::GUS-mCit* and *IQD22::GUS-mCit* lines were constructed by Carl Procko (Procko et al. 2022) and were crossed with MCabi#2 to generate lines with ABA-insensitive, labeled spongy or palisade MC. We labeled the bundle sheath by crossing BSabi#14 with *SCR::GFP* (Torne et al. 2021). All primers and vectors used in this work are summarized in Supplemental Table S2.

Arabidopsis plants were grown in 250-mL pots, with 2 to 3 plants in each pot. Those pots were filled with soil (Klasmann686, Klasmann-Deilmann, Germany) + 4 g/L Osmocote 6M. The potted plants were kept in a growth chamber at 22 °C and 70% relative humidity, with an 8-h light (09:00 to 17:00)/16-h dark photoperiod (short day). During the day, the illumination, humidity, and VPD changed in a pattern resembling natural conditions, as in Negin and Moshelion (2017). The illumination intensity provided by LED light strips (EnerLED 24 V-5630, 24 W/m, 3000 K [50%]/6000 K [50%]) reached 150 to 200 μmol m^{-2} s^{-1} at the plant level at midday.

The FBPase::*abi1-1* and SCR::*abi1-1* constructs and plant transformation

For construct assembly, the MultiSite Gateway Three-Fragment Vector Construction Kit (Invitrogen, Ghent, Belgium) was used according to the manufacturer's instructions. The construction of the MCabi plants with ABA-insensitive mesophyll is described in Negin et al. (2019). (In that work, the MCabi plants are referred as *fa* plants.) Briefly, the *abi1-1* gene (Koornneef et al. 1984) and the FBPase promoter (Lloyd et al. 1991) were cloned into pDONR plasmids and then inserted into the binary pB7M24GW (Invitrogen) plasmid. As MC and BSC are connected by plasmodesmata, we cannot exclude the diffusion of mutated *abi1-1* genes from MC to BSC. Therefore, we considered MCabi plants to be ABA-insensitive in their MC and BSC. The plants with ABA-insensitive BSC (BSabi plants) were constructed in the same way, using the SCR (Shatil-Cohen et al. 2011) promoter, which has been observed in the BSC associated with all veins in mature leaves (Wysocka-Diller et al. 2000). We cannot rule out the diffusion of *abi1-1* into other tissues in the BSabi plants, yet the strongest effect of *abi1-1* is expected at the site at where it is expressed. The dominance of the *abi1-1* mutation is due to its "gain of function" nature, negatively regulating ABA signaling (Gosti et al. 1999), with only 9% of the ABA-responsive genes remaining unaltered in *abi1-1* plants (Hoth et al. 2002). As such, it has a quantity-dependent attribute (high phosphatase activity represses the phosphorylation of SnRKs and, consequently, the initiation of ABA signal transduction). In our plants, *abi1-1* was constitutively expressed under a nonnative promotor, in addition to the native ABI1 and other PP2Cs expression, suppressing ABA signaling. Therefore, we expected that its strongest effect would be seen at its expression site. Having said that, the dominance could be trait-dependent (Finkelstein 1994; Leung et al. 1997), and, therefore, we always compared the *abi1-1* phenotype with the WT control.

Binary plasmids were floral-dipped (Clough and Bent 1998). The presence of the transgene containing the G to A substitution was confirmed by sequencing and NocI digestion (described below). The study was performed on 3 independent lines of each construct, using homozygous t_3 and t_4 lines.

Characterization of transgenic plants

Stomatal aperture and index

Stomatal aperture and index were measured as described by Yaaran et al. (2019). Briefly, epidermal peels were soaked in

closure solutions under light (~150 μmol m^{-2} s^{-1}). After 1.5 h, ABA ([+]-*cis*, *trans*-ABA; Biosynth, Staad, Switzerland) was added to reach a concentration of 10 μM. DMSO at the same concentration was added to the control. All stomata were photographed under a bright-field inverted microscope (1M7100, Zeiss, Jena, Germany) on which a Hitachi HV-D30 CCD camera (Hitachi, Tokyo, Japan) was mounted. Stomatal images were analyzed to determine aperture size using the ImageJ software. Stomatal index was calculated as the number of stomata/number of epidermal cells in an area of 2 mm^2.

Leaf vein density, area and cross sections

Leaf vein density was measured as described by Grunwald (2021). Briefly, leaves of the same age and size as those used in the K_{leaf} assay were immersed in 96% (*v*/*v*) ethanol solution and incubated at 50 °C. The used ethanol was replaced with fresh ethanol until leaves were completely colorless and then was finally replaced with 88% (*v*/*v*) lactic acid solution (Fischer Scientific, UK) for overnight incubation at room temperature. Then, the leaves were rinsed in water and submerged in 0.5% (*w*/*v*) safranin O dissolved in water (Sigma Aldrich cat. no S2255) for 1 min, followed by an overnight incubation in water to remove any excess dye. Then, the leaves were scanned in a water tray using an Epson 12000XL scanner (Seiko Epson, Japan) with a 2,500-dpi resolution, and 2 to 3 patches (~1 cm^2 each) for each leaf (9 to 10 leaves per line) were analyzed using WinRhizo software (https://regent.qc.ca/assets/winrhizo_about.html) for vein detection. Vein density was calculated by dividing the total vein length by the total leaf area scanned.

Leaf area is the projected area of a fully expanded leaf (average of 5 leaves from each plant and 6 plants of each of the 3 independent lines of MCabi and BSabi). Leaf area was assessed using the LI-3100C Area Meter (https://www.licor.com/env/).

Leaf cross sections for anatomical analysis of the veins and mesophyll were free-hand cut using a sharp scalpel. Then, the cross sections were cleared using ClearSee (Kurihara et al. 2015) and stained in a 1-min incubation in Toluidine Blue O dissolved in water (TB; cat. no. T-3260, https://www.sigmaaldrich.com). They were then washed with water 2 or 3 times. Cross sections were photographed in the same setup as that used for the analyses of stomatal aperture and index. ImageJ software was used to analyze the images to determine mesophyll length.

Leaf gas-exchange and hydraulic-conductance (K_{leaf}) measurements

Gas exchange and hydraulic conductance were measured as described by Negin et al. (2019), using leaves of 6- to 8-wk-old plants grown under short-day conditions. Briefly, 2 leaves from each plant were excised before dawn and put into tubes containing artificial xylem sap (AXS; Shatil-Cohen et al. 2011) and 0.01% (*v*/*v*) DMSO (control) or 10 μM ABA. The leaves were then put into hermetically sealed transparent boxes and left in the light for a minimum of 1 h. Following that period, the lids were opened for 15 min, after which time gas exchange was measured using the LI-6400xt portable gas-exchange system equipped with the *Arabidopsis* chamber (LI-COR, Inc., Lincoln, NE, USA). Chamber conditions were set to 400 ppm CO_2, PAR of 200 μmol m^{-2} s^{-1}, VPD of ~1.2 kPa and flow of 200 μmol s^{-1}. In the enclosed gas-exchange chamber, there is a trade-off between the stability of humidity vs. stability of the flow. We choose to keep the flow constant at the expense of humidity stability, to maintain an undisturbed boundary layer.

Immediately following the gas-exchange measurement, the leaf was transferred to a pressure chamber (ARIMAD-3000, MRC, Israel) to measure Ψ_{leaf} and determine K_{leaf} (Sade et al. 2014). K_{leaf} was calculated for each individual leaf by dividing the leaf transpiration rate, E, by the water potential gradient across the leaf (Martre et al. 2002; Sack and Holbrook 2006). As the leaf petiole was dipped in AXS at a water potential of −0.027 MPa, the water potential gradient equaled $-0.027 - \Psi_{leaf}$, which we simplified as $-\Psi_{leaf}$ in our calculation. These measurements were conducted between 10:00 and 13:00 (1 to 4 h after the lights were turned on).

Whole-plant continuous transpiration

The whole-plant continuous transpiration rate was measured using a high-throughput telemetric, gravimetric-based phenotyping system (Plantarry 3.0 system, Plant-DiTech, Israel; Dalal et al. 2020) in the greenhouse of the I-CORE Center for Functional Phenotyping (http://departments.agri.huji.ac.il/plantscience/icore.phpon) as described in (Yaaran et al. 2019; Dalal et al. 2020). The output (weight) of the load cells was monitored every 3 min and analyzed using SPAC analytics (Plant-Ditech). Seedlings were transferred to 1.6-L pots (4 plants per pot) and gradually exposed to semi-controlled greenhouse conditions: 24 to 9 °C (day/night) and the natural day length and light conditions prevailing in Rehovot, Israel, during December and January of 2021.

After establishment, each pot was placed on a load cell in a randomized block arrangement. Daily measurements were conducted continuously and simultaneously for all of the plants in the array, so that all of the plants were exposed to similar ambient conditions at each measurement point. The soil surface surrounding each *Arabidopsis* plant was covered, as well as the crack between the pot and load cell, to prevent evaporation. The transpiration rate was normalized to the total plant weight to determine E, as described in Halperin et al. (2017) and Yaaran et al. (2019).

Protoplast isolation and measurement of the membrane osmotic water permeability coefficient (P_f)

Protoplast isolation and measurements of the osmotic water permeability coefficient (P_f) were performed as described by Shatil-Cohen et al. (2014). In brief, protoplasts were isolated from 6- to 8-wk-old plants according to the gentle and rapid (<30 min) method using an isotonic solution in the extraction process (pH 5.7, 600 mOsmol). For the ABA treatment,

protoplasts were incubated in 1 μM ABA for 1 to 4 h. We observed the protoplasts swelling in response to the hypoosmotic challenge (of 0.37 MPa) generated by changing the bath solutions from isotonic (600 mOsmol) to hypotonic (450 mOsmol). Palisade and spongy mesophyll protoplasts were identified by *mCit* fluorescence. Protoplasts were recorded using an inverted epifluorescent microscope (Nikon Eclipse TS100) with a 20×/NA 0.40 objective, a CCD 12-bit camera Manta G-235B (https://www.alliedvision.com) and image-processing software (AcquireControl v5.0.0; https://www.alliedvision.com). P_f was determined based on the rate at which cell volume increased for 60 s starting from the hypoosmotic challenge, using a numerical approach in an offline curve-fitting procedure of the PfFit program.

Relative symplastic permeability

DANS assays were performed as described by Cui and Lee (2016) with minimal modifications. In brief, 2 1-μL droplets of 2 mM 5(6)-carboxyfluorescein diacetate (CFDA; cat. #19582 https://www.caymanchem.com) were loaded on the center of the adaxial surface of a mature leaf from a 7- to 8-wk-old plant. This was followed by inverted epifluorescent microscope imaging (described above for the P_f measurements) of the abaxial surface of the leaf at 10 min after loading. The nonfluorescent ester CFDA can cross cell membranes passively in its electrically neutral or near-neutral form. Once inside the cells, it is subject to cleavage by esterases to form a polar fluorescent compound, CF. The extent of cell-to-cell dye movement is expected to represent the permeability of the plasmodesmata and was evaluated using an intensity distance chart that was analyzed using ImageJ. A magnification of 10× was used, despite the fact that the size of some of the MCabi samples exceeded the imaging border (maximum of 388% compared to WT under control conditions), in order to capture the extent of all lines' cell-to-cell fluorescence under the same imaging conditions. The average of the 2 droplets was considered the leaf's DANS measurement.

Both attached and detached leaf measurements were performed between 10:00 and 14:00. The detached leaf experimental setup was like the setup used for the measurements of hydraulic conductivity (K_{leaf}).

Statistical analysis

The data were analyzed using Student's *t*-test for comparisons of 2 means and Tukey's honestly significant difference (HSD) test for comparisons of more than 2 means. When 2 variables were examined (e.g. line and ABA treatment), the interaction between those factors was evaluated using a 2-way ANOVA, followed by Tukey's HSD test. The model effects and different *P*-values attained from the 2-way ANOVAs are presented in Supplemental Table S1. All analyses were done with JMP software (SAS, Cary, NC, USA)

Accession Numbers

Accession numbers of major genes mentioned in this paper are FBPase promoter, AR390745; SCARECROW (SCR) promoter, AT3G54220; *abi1-1*, AT4G26080.1 polymorphism 4769512; IQD22, AT4G23060; CORI3, AT4G23600.

Acknowledgments

We thank Jung-Youn Lee for generously providing us with the *CalS8-1* (037603C) line. We thank Dr. Julius Ben-Ari for the LC-MS/MS analyses of ABA samples and Eduard Belausov for the confocal imaging.

Author contributions

A.Y. designed and performed the research, analyzed the data, formulated the hypotheses, and wrote the manuscript. E.E. contributed to the characterization of transgenic plants and the P_f measurements. C.P. constructed and validated the *CORI3::GUS-mCit* and *IQD22::GUS-mCit* lines. M.M. (the corresponding author) formulated the hypotheses and wrote the manuscript together with A.Y.

Supplemental data

Supplemental Fig. S1. Characterization of BSabi plants.

Supplemental Fig. S2. ABA and salicylic acid levels of MCabi and BSabi.

Supplemental Fig. S3. Leaf hydraulic conductance (K_{leaf}) of the 3 independent lines of MCabi and BSabi plants.

Supplemental Fig. S4. Transgenes high transpiration reduced the VPD in the small gas-exchange chamber.

Supplemental Fig. S5. Continuous whole-plant data collected under greenhouse conditions throughout the experiment.

Supplemental Fig. S6. Gas-exchange measurements of mutants with impaired plasmodesmatal permeability.

Supplemental Fig. S7. The symplastic pathway's response to ABA.

Supplemental Fig. S8. Validation of measurements of symplastic permeability.

Supplemental Table S1. Results of the 2-way ANOVA.

Supplemental Table S2. List of primers and vectors used in this work.

Funding

This research was supported by the Israel Science Foundation (Grant No. 1043/20) and NIH (Grant No. 5R35GM122604).

Conflict of interest statement. None declared.

References

Ache P, Bauer H, Kollist H, Al-Rasheid KAS, Lautner S, Hartung W, Hedrich R. Stomatal action directly feeds back on leaf turgor: new insights into the regulation of the plant water status from non-invasive pressure probe measurements. Plant J. 2010:**62**(6): 1072–1082. https://doi.org/10.1111/j.1365-313X.2010.04213.x

Álvarez-Arenas TEG, Sancho-Knapik D, Peguero-Pina JJ, Gómez-Arroyo A, Gil-Pelegrín E. Non-contact ultrasonic resonant spectroscopy resolves the elastic properties of layered plant tissues. Appl Phys Lett. 2018:**113**(25):253704. https://doi.org/10.1063/1.5064517

Amsbury S, Kirk P, Benitez-Alfonso A. Emerging models on the regulation of intercellular transport by plasmodesmata-associated callose. J Exp Bot. 2017:**69**:105–115

Attia Z, Dalal A, Moshelion M. Vascular bundle sheath and mesophyll cells modulate leaf water balance in response to chitin. Plant J. 2019:**101**(6):1368–1377. https://doi.org/10.1111/tpj.14598

Bacete L, Schulz J, Engelsdorf T, Bartosova Z, Vaahtera L, Yan G, Gerhold JM, Ticha T, Øvstebø C, Gigli-Bisceglia N, et al. THESEUS1 Modulates cell wall stiffness and abscisic acid production in *Arabidopsis thaliana*. Proc Natl Acad Sci U S A. 2022:**119**(1):e2119258119. https://doi.org/10.1073/pnas.2119258119

Blackman CJ, Brodribb TJ, Jordan GJ. Leaf hydraulics and drought stress: response, recovery and survivorship in four woody temperate plant species. Plant Cell Environ. 2009:**32**(11):1584–1595. https://doi.org/10.1111/j.1365-3040.2009.02023.x

Blackman CJ, Brodribb TJ, Jordan GJ. Leaf hydraulic vulnerability is related to conduit dimensions and drought resistance across a diverse range of woody angiosperms. New Phytol. 2010:**188**(4):1113–1123. https://doi.org/10.1111/j.1469-8137.2010.03439.x

Blum A. Effective use of water (EUW) and not water-use efficiency (WUE) is the target of crop yield improvement under drought stress. F Crop Res. 2009:**112**(2-3):119–123. https://doi.org/10.1016/j.fcr.2009.03.009

Brodribb TJ, Feild TS, Jordan GJ. Leaf Maximum photosynthetic rate and venation are linked by hydraulics. Plant Physiol. 2007:**144**(4):1890–1898. https://doi.org/10.1104/pp.107.101352

Brodribb TJ, Feild TS, Sack L. Viewing leaf structure and evolution from a hydraulic perspective. Funct Plant Biol. 2010:**37**(6):488–498. https://doi.org/10.1071/FP10010

Brodribb TJ, Holbrook NM, Zwieniecki MA, Palma B. Leaf hydraulic capacity in ferns, conifers and angiosperms: impacts on photosynthetic maxima. New Phytol. 2005:**165**(3):839–846. https://doi.org/10.1111/j.1469-8137.2004.01259.x

Buckley TN. The contributions of apoplastic, symplastic and gas phase pathways for water transport outside the bundle sheath in leaves. Plant. Cell Environ. 2015:**38**(1):7–22. https://doi.org/10.1111/pce.12372

Buckley TN, John GP, Scoffoni C, Sack L. How does leaf anatomy influence water transport outside the xylem? Plant Physiol. 2015:**168**(4):1616–1635. https://doi.org/10.1104/pp.15.00731

Canny M. Water loss from leaf mesophyll stripped of the epidermis. Funct Plant Biol. 2012:**39**(5):421–434. https://doi.org/10.1071/FP11265

Canny M, Wong SC, Huang C, Miller C. Differential shrinkage of mesophyll cells in transpiring cotton leaves: implications for static and dynamic pools of water, and for water transport pathways. Funct Plant Biol. 2012:**39**(2):91–102. https://doi.org/10.1071/FP11172

Caringella MA, Bongers FJ, Sack L. Leaf hydraulic conductance varies with vein anatomy across *Arabidopsis thaliana* wild-type and leaf vein mutants. Plant Cell Environ. 2015:**38**:2735–46. https://doi.org/10.1111/pce.12584

Clough SJ, Bent AF. Floral dip: a simplified method for *Agrobacterium*-mediated transformation of *Arabidopsis thaliana*. Plant J. 1998:**16**(6):735–743. https://doi.org/10.1046/j.1365-313x.1998.00343.x

Cochard H, Venisse JS, Barigah TS, Brunel N, Herbette S, Guilliot A, Tyree MT, Sakr S. Putative role of aquaporins in variable hydraulic conductance of leaves in response to light. Plant Physiol. 2007:**143**(1):122–133. https://doi.org/10.1104/pp.106.090092

Coupel-Ledru A, Tyerman SD, Masclef D, Lebon E, Christophe A, Edwards EJ, Simonneau T. Abscisic acid down-regulates hydraulic conductance of grapevine leaves in isohydric genotypes only. Plant Physiol. 2017:**175**(3):1121–1134. https://doi.org/10.1104/pp.17.00698

Cui W, Lee JY. *Arabidopsis* callose synthases CalS1/8 regulate plasmodesmal permeability during stress. Nat Plants. 2016:**2**(5):16034. https://doi.org/10.1038/NPLANTS.2016.34

Dalal A, Shenhar I, Bourstein R, Mayo A, Grunwald Y, Averbuch N, Attia Z, Wallach R, Moshelion M. A telemetric, gravimetric platform for real-time physiological phenotyping of plant–environment interactions. J Vis Exp. 2020:(162). https://doi.org/10.3791/61280

de Wit C. Transpiration and crop yields. Versl Landbouwk Onderz. 1958:**64**(6):18–20

Erwee MG, Goodwin PB. Characterization of the *Egeria densa* leaf symplast: response to plasmolysis, deplasmolysis and to aromatic amino acids. Protoplasma 1984:**122**(3):162–168. https://doi.org/10.1007/BF01281693

Finkelstein RR. Maternal effects govern variable dominance of two abscisic acid response mutations in *Arabidopsis thaliana*. Plant Physiol. 1994:**105**(4):1203–1208. https://doi.org/10.1104/pp.105.4.1203

Fischer RA, Rees D, Sayre KD, Lu ZM, Condon AG, Larque Saavedra A. Wheat yield progress associated with higher stomatal conductance and photosynthetic rate, and cooler canopies. Crop Sci. 1998:**38**(6):1467–1475. https://doi.org/10.2135/cropsci1998.0011183X003800060011x

Galvez-Valdivieso G, Fryer MJ, Lawson T, Slattery K, Truman W, Smirnoff N, Asami T, Davies WJ, Jones AM, Baker NR, et al. The high light response in *Arabidopsis* involves ABA signaling between vascular and bundle sheath cells. Plant Cell 2009:**21**(7):2143–2162. https://doi.org/10.1105/tpc.108.061507

Gosti F, Beaudoin N, Serizet C, Webb AAR, Vartanian N, Giraudat J. ABI1 protein phosphatase 2C is a negative regulator of abscisic acid signaling. Plant Cell 1999:**11**(10):1897–1910. https://doi.org/10.1105/tpc.11.10.1897

Griffiths H, Weller G, Toy LFM, Dennis RJ. You're so vein: bundle sheath physiology, phylogeny and evolution in C3 and C4 plants. Plant Cell Environ. 2013:**36**(2):249–261. https://doi.org/10.1111/j.1365-3040.2012.02585.x

Grondin A, Rodrigues O, Verdoucq L, Merlot S, Leonhardt N, Maurel C. Aquaporins contribute to ABA-triggered stomatal closure through OST1-mediated phosphorylation. Plant Cell 2015:**27**(7):1945–1954. https://doi.org/10.1105/tpc.15.00421

Grunwald Y, Gosa SC, Torne-Srivastava T, Moran N, Moshelion M. Out of the blue: phototropins of the leaf vascular bundle sheath mediate the regulation of leaf hydraulic conductance by blue light. Plant Cell 2022;**34**(6):2328–2342. https://doi.org/10.1093/plcell/koac089

Grunwald Y, Wigoda N, Sade N, Yaaran A, Torne T, Gosa SC, Moran N, Moshelion M. *Arabidopsis* leaf hydraulic conductance is regulated by xylem sap pH, controlled, in turn, by a P-type H^+-ATPase of vascular bundle sheath cells. Plant J. 2021:**6**(2):301–313. https://doi.org/10.1111/tpj.15235

Halperin O, Gebremedhin A, Wallach R, Moshelion M. High-throughput physiological phenotyping and screening system for the characterization of plant-environment interactions. Plant J. 2017:**89**(4):839–850. https://doi.org/10.1111/tpj.13425

Hoth S, Morgante M, Sanchez JP, Hanafey MK, Tingey SV, Chua NH. Genome-wide gene expression profiling in *Arabidopsis thaliana* reveals new targets of abscisic acid and largely impaired gene regulation in the *abi1-1* mutant. J Cell Sci. 2002:**115**(24):4891–4900. https://doi.org/10.1242/jcs.00175

Iino M, Ogawa T, Zeiger E. Kinetic properties of the blue-light response of stomata. Proc Natl Acad Sci U S A. 1985:**82**(23):8019–8023. https://doi.org/10.1073/pnas.82.23.8019

Kelly G, Sade N, Doron-Faigenboim A, Lerner S, Shatil-Cohen A, Yeselson Y, Egbaria A, Kottapalli J, Schaffer AA, Moshelion M, et al. Sugar and hexokinase suppress expression of PIP aquaporins and reduce leaf hydraulics that preserves leaf water potential. Plant J. 2017:**91**(2):325–339. https://doi.org/10.1111/tpj.13568

Kemanian AR, Stöckle CO, Huggins DR. Transpiration-use efficiency of barley. Agric For Meteorol. 2005:**130**(1-2):1–11. https://doi.org/10.1016/j.agrformet.2005.01.003

Kim YX, Steudle E. Light and turgor affect the water permeability (aquaporins) of parenchyma cells in the midrib of leaves of *Zea mays*. J Exp Bot. 2007:**58**(15-16):4119–4129. https://doi.org/10.1093/jxb/erm270

Kim YX, Steudle E. Gating of aqaporins by light and reactive oxygen species in leaf parenchyma cells of the midrib of *Zea mays*. J Exp Bot. 2009:**60**(2):547–556. https://doi.org/10.1093/jxb/ern299

Kitagawa M, Tomoi T, Fukushima T, Sakata Y, Sato M, Toyooka K, Fujita T, Sakakibara H. Abscisic acid acts as a regulator of molecular trafficking through plasmodesmata in the moss *Physcomitrella patens*. Plant Cell Physiol. 2019:**60**(4):738–751. https://doi.org/10.1093/pcp/pcy249

Koornneef M, Reuling G, Karssen CM. The isolation and characterization of abscisic acid-insensitive mutants of *Arabidopsis thaliana*. Physiol Plant. 1984:**61**(3):377–383. https://doi.org/10.1111/j.1399-3054.1984.tb06343.x

Kurihara D, Mizuta Y, Sato Y, Higashiyama T. Clearsee: a rapid optical clearing reagent for whole-plant fluorescence imaging. Development 2015:**142**(23):4168–4179. https://doi.org/10.1242/dev.127613

Leegood RC. Roles of the bundle sheath cells in leaves of C3 plants. J Exp Bot. 2008:**59**(7):1663–1673. https://doi.org/10.1093/jxb/erm335

Leung J, Merlot S, Giraudat J. The *Arabidopsis* ABSCISIC ACID-INSENSITIVE2 (ABI2) and ABI1 genes encode homologous protein phosphatases 2C involved in abscisic acid signal transduction. Plant Cell 1997:**9**(5):759–771. https://doi.org/10.1105/tpc.9.5.759

Lloyd JC, Raines CA, John UP, Dyer TAA. The chloroplast FBPase gene of wheat: structure and expression of the promoter in photosynthetic and meristematic cells of transgenic tobacco plants. Mol Gen Genet. 1991:**225**(2):209–216. https://doi.org/10.1007/BF00269850

Manohar M, Wang D, Manosalva PM, Choi HW, Kombrink E, Klessig DF. Members of the abscisic acid co-receptor PP2C protein family mediate salicylic acid-abscisic acid crosstalk. Plant Direct. 2017:**1**(5):e00020. https://doi.org/10.1002/pld3.20

Martre P, Morillon R, Barrieu F, North GB, Nobel PS, Chrispeels MJ. Plasma membrane aquaporins play a significant role during recovery from water deficit. Plant Physiol. 2002:**130**(4):2101–2110. https://doi.org/10.1104/pp.009019

Maurel C. Aquaporins and water permeability of plant membranes. Annu Rev Plant Biol. 1997:**48**(1):399–429. https://doi.org/10.1146/annurev.arplant.48.1.399

McAdam SAM, Brodribb TJ. Linking turgor with ABA biosynthesis: implications for stomatal responses to vapor pressure deficit across land plants. Plant Physiol. 2016:**171**(3):2008–2016. https://doi.org/10.1104/pp.16.00380

Merilo E, Yarmolinsky D, Jalakas P, Parik H, Tulva I, Rasulov B, Kilk K, Kollist H. Stomatal VPD response: there is more to the story than ABA. Plant Physiol. 2018:**176**(1):851–864. https://doi.org/10.1104/pp.17.00912

Morillon R, Chrispeels MJ. The role of ABA and the transpiration stream in the regulation of the osmotic water permeability of leaf cells. Proc Natl Acad Sci U S A. 2001:**98**(24):14138–14143. https://doi.org/10.1073/pnas.231471998

Mott KA, Parkhurst DF. Stomatal responses to humidity in air and helox. Plant, Cell Environ. 1991:**14**(5):509–515. https://doi.org/10.1111/j.1365-3040.1991.tb01521.x

Muries B, Mom R, Benoit P, Brunel-michac N, Cochard H, Drevet P, Petel G, Badel E, Fumanal B, Gousset-dupont A, et al. Aquaporins and water control in drought-stressed poplar leaves: a glimpse into the extraxylem vascular territories. Environ Exp Bot. 2019:**162**:25–37. https://doi.org/10.1016/j.envexpbot.2018.12.016

Nardini A, Gortan E, Salleo S. Hydraulic efficiency of the leaf venation system in sun- and shade-adapted species. Funct Plant Biol. 2005:**32**(10):953–961. https://doi.org/10.1071/FP05100

Nardini A, Raimondo F, Lo Gullo MA, Salleo S. Leafminers help us understand leaf hydraulic design. Plant Cell Environ. 2010:**33**(7):1091–1100. https://doi.org/10.1111/j.1365-3040.2010.02131.x

Nardini A, Salleo S, Andri S. Circadian regulation of leaf hydraulic conductance in sunflower (Helianthus annuus L. cv Margot). Plant Cell Environ. 2005b:**28**(6):750–759. https://doi.org/10.1111/j.1365-3040.2005.01320.x

Negin B, Moshelion M. The advantages of functional phenotyping in pre-field screening for drought-tolerant crops. Funct Plant Biol. 2017:**44**(1):107–118. https://doi.org/10.1071/FP16156

Negin B, Yaaran A, Kelly G, Zait Y, Moshelion M. Mesophyll abscisic acid restrains early growth and flowering but does not directly suppress photosynthesis. Plant Physiol. 2019:**180**(2):910–925. https://doi.org/10.1104/pp.18.01334

Pantin F, Monnet F, Jannaud D, Costa JM, Renaud J, Muller B, Simonneau T, Genty B. The dual effect of abscisic acid on stomata. New Phytol. 2013:**197**(1):65–72. https://doi.org/10.1111/nph.12013

Pilot G, Stransky H, Bushey D. Overexpression of GLUTAMINE DUMPER1 leads to hypersecretion of glutamine from hydathodes of *Arabidopsis* leaves. Plant Cell. 2004:**16**(7):1827–1840. https://doi.org/10.1105/tpc.021642

Pou A, Medrano H, Flexas J, Tyerman SD. A putative role for TIP and PIP aquaporins in dynamics of leaf hydraulic and stomatal conductances in grapevine under water stress and re-watering. Plant. Cell Environ. 2013:**36**(4):828–843. https://doi.org/10.1111/pce.12019

Prado K, Boursiac Y, Tournaire-Roux C, Monneuse J-M, Postaire O, Da Ines O, Schäffner AR, Hem S, Santoni V, Maurel C. Regulation of *Arabidopsis* leaf hydraulics involves light-dependent phosphorylation of aquaporins in veins. Plant Cell 2013:**25**(3):1029–1039. https://doi.org/10.1105/tpc.112.108456

Prado K, Maurel C. Regulation of leaf hydraulics: from molecular to whole plant levels. Front Plant Sci. 2013:**4**:255. https://doi.org/10.3389/fpls.2013.00255

Procko C, Lee T, Borsuk A, Bargmann BOR, Dabi T, Nery JR, Estelle M, Baird L, O'Connor C, Brodersen C, et al. Leaf cell-specific and single-cell transcriptional profiling reveals a role for the palisade layer in UV light protection. Plant Cell 2022:**34**(9):3261–3279. https://doi.org/10.1093/plcell/koac167

Richards RA. Selectable traits to increase crop photosynthesis and yield of grain crops. J Exp Bot. 2000:**51 Spec No**:447–458. https://doi.org/10.1093/jexbot/51.suppl_1.447

Roberts IM, Boevink P, Roberts AG, Sauer N, Reichel C, Oparka KJ. Dynamic changes in the frequency and architecture of plasmodesmata during the sink-source transition in tobacco leaves. Protoplasma 2001:**218**(1-2):31–44. https://doi.org/10.1007/BF01288358

Rockwell FE, Holbrook NM, Stroock AD. The competition between liquid and vapor transport in transpiring leaves. Plant Physiol. 2014:**164**(4):1741–1758. https://doi.org/10.1104/pp.114.236323

Sack L, Holbrook NM. Leaf hydraulics. Annu Rev Plant Biol. 2006:**57**(1):361–381. https://doi.org/10.1146/annurev.arplant.56.032604.144141

Sack L, John GP, Buckley TN. ABA accumulation in dehydrating leaves is associated with decline in cell volume, not turgor pressure. Plant Physiol. 2018:**176**(1):489–493. https://doi.org/10.1104/pp.17.01097

Sade N, Shatil-Cohen A, Attia Z, Maurel C, Boursiac Y, Kelly G, Granot D, Yaaran A, Lerner S, Moshelion M. The role of plasma membrane aquaporins in regulating the bundle sheath-mesophyll continuum and leaf hydraulics. Plant Physiol. 2014:**166**(3):1609–1620. https://doi.org/10.1104/pp.114.248633

Sade N, Shatil-Cohen A, Moshelion M. Bundle-sheath aquaporins play a role in controlling *Arabidopsis* leaf hydraulic conductivity. Plant Signal Behav. 2015:**10**(5):1–4. https://doi.org/10.1080/15592324.2015.1017177

Schulz A. Plasmodesmal widening accompanies the short-term increase in symplasmic phloem unloading in pea root tips under osmotic stress. Protoplasma 1995:**188**(1-2):22–37. https://doi.org/10.1007/BF01276793

Scoffoni C, Albuquerque C, Brodersen CR, Townes S V, John GP, Bartlett MK, Buckley TN, McElrone AJ, Sack L. Outside-xylem vulnerability, not xylem embolism, controls leaf hydraulic decline during dehydration. Plant Physiol. 2017:**173**(2):1197–1210. https://doi.org/10.1104/pp.16.01643

Scoffoni C, Rawls M, Mckown A, Cochard H, Sack L. Decline of leaf hydraulic conductance with dehydration: relationship to leaf size

and venation architecture. Plant Physiol. 2011:**156**(2):832–843. https://doi.org/10.1104/pp.111.173856

Scoffoni C, Sack L. The causes and consequences of leaf hydraulic decline with dehydration. J Exp Bot. 2017:**68**(16):4479–4496. https://doi.org/10.1093/jxb/erx252

Scoffoni C, Vuong C, Diep S, Cochard H, Sack L. Leaf shrinkage with dehydration: coordination with hydraulic vulnerability and drought tolerance. Plant Physiol. 2014:**164**(4):1772–1788. https://doi.org/10.1104/pp.113.221424

Shapira O, Khadka S, Israeli Y, Shani U, Schwartz A. Functional anatomy controls ion distribution in banana leaves: significance of Na+ seclusion at the leaf margins. Plant Cell Environ. 2009:**32**(5):476–485. https://doi.org/10.1111/j.1365-3040.2009.01941.x

Shatil-Cohen A, Attia Z, Moshelion M. Bundle-sheath cell regulation of xylem-mesophyll water transport via aquaporins under drought stress: a target of xylem-borne ABA? Plant J. 2011:**67**(1):72–80. https://doi.org/10.1111/j.1365-313X.2011.04576.x

Shatil-Cohen A, Moshelion M. The bundle sheath role as xylem-mesophyll barrier. Plant Signal Behav. 2012:**7**(9):1088–1091. https://doi.org/10.4161/psb.21162

Shatil-Cohen A, Sibony H, Draye X, Chaumont F, Moran N, Moshelion M. Measuring the osmotic water permeability coefficient (pf) of spherical cells: isolated plant protoplasts as an example. J Vis Exp. 2014:(92):e51652. https://doi.org/10.3791/51652

Shivaraj SM, Sharma Y, Chaudhary J, Rajora N, Sharma S, Thakral V, Ram H, Sonah H, Singla-Pareek SL, Sharma TR, et al. Dynamic role of aquaporin transport system under drought stress in plants. Environ Exp Bot. 2021:**184**:104367. https://doi.org/10.1016/j.envexpbot.2020.104367

Sinclair TR. Effective water use required for improving crop growth rather than transpiration efficiency. Front Plant Sci. 2018:**9**:1442. https://doi.org/10.3389/fpls.2018.01442

Sperry JS, Venturas MD, Anderegg WRL, Mencuccini M, Mackay DS, Wang Y, Love DM. Predicting stomatal responses to the environment from the optimization of photosynthetic gain and hydraulic cost. Plant Cell Environ. 2017:**40**(6):816–830. https://doi.org/10.1111/pce.12852

Steudle E, Peterson CA. How does water get through roots? J Exp Bot. 1998:**49**(322):775–788. https://doi.org/10.1093/jxb/49.322.775

Sussmilch FC, Brodribb TJ, McAdam SAM. Up-regulation of NCED3 and ABA biosynthesis occur within minutes of a decrease in leaf turgor but AHK1 is not required. J Exp Bot. 2017:**68**(11):2913–2918. https://doi.org/10.1093/jxb/erx124

Tholen D, Boom C, Zhu XG. Opinion: prospects for improving photosynthesis by altering leaf anatomy. Plant Sci. 2012:**197**:92–101. https://doi.org/10.1016/j.plantsci.2012.09.005

Torne T, Grunwald Y, Dalal A, Yaaran A, Moshelion M, Moran N. Stress is basic: ABA alkalinizes both the xylem sap and the cytosol by inhibiting their P-type H^+-ATPase and stimulating their V-type H^+-ATPase. bioRxiv 2021.03.24.436813. 2021.

Tylewicz S, Petterle A, Marttila S, Miskolczi P, Azeez A, Singh RK, Immanen J, Mähler N, Hvidsten TR, Eklund DM, et al. Photoperiodic control of seasonal growth is mediated by ABA acting on cell-cell communication. Science 2018:**360**(6385):212–215. https://doi.org/10.1126/science.aan8576

Tyree MT, Nardini A, Salleo S, Sack L, El Omari B. The dependence of leaf hydraulic conductance on irradiance during HPFM measurements: any role for stomatal response? J Exp Bot. 2005:**56**(412):737–744. https://doi.org/10.1093/jxb/eri045

Voicu MC, Cooke JEK, Zwiazek JJ. Aquaporin gene expression and apoplastic water flow in bur oak (*Quercus macrocarpa*) leaves in relation to the light response of leaf hydraulic conductance. J Exp Bot. 2009:**60**(14):4063–4075. https://doi.org/10.1093/jxb/erp239

Wang X, Sager R, Cui W, Zhang C, Lu H, Lee JY. Salicylic acid regulates plasmodesmata closure during innate immune responses in *Arabidopsis*. Plant Cell 2013:**25**(6):2315–2329. https://doi.org/10.1105/tpc.113.110676

Wysocka-Diller JW, Helariutta Y, Fukaki H, Malamy JE, Benfey PN. Molecular analysis of SCARECROW function reveals a radial patterning mechanism common to root and shoot. Development 2000:**127**(3):595–603. https://doi.org/10.1242/dev.127.3.595

Xiong D, Nadal M. Linking water relations and hydraulics with photosynthesis. Plant J. 2020:**101**(4):800–815. https://doi.org/10.1111/tpj.14595

Yaaran A, Moshelion M. Role of aquaporins in a composite model of water transport in the leaf. Int J Mol Sci. 2016:**17**(7):1045. https://doi.org/10.3390/ijms17071045

Yaaran A, Negin B, Moshelion M. Plant science role of guard-cell ABA in determining steady-state stomatal aperture and prompt vapor-pressure-deficit response. Plant Sci. 2019:**281**:31–40. https://doi.org/10.1016/j.plantsci.2018.12.027

Yoo CY, Pence HE, Hasegawa PM, Mickelbart M V. Regulation of transpiration to improve crop water use. CRC Crit Rev Plant Sci. 2009:**28**(6):410–431. https://doi.org/10.1080/07352680903173175

Yoshida T, Christmann A, Yamaguchi-Shinozaki K, Grill E, Fernie AR. Revisiting the basal role of ABA—roles outside of stress. Trends Plant Sci. 2019:**24**(7):625–635. https://doi.org/10.1016/j.tplants.2019.04.008

Zait Y, Shapira O, Schwartz A. The effect of blue light on stomatal oscillations and leaf turgor pressure in banana leaves. Plant Cell Environ. 2017:**40**(7):1143–1152. https://doi.org/10.1111/pce.12907

Zavaliev R, Levy A, Gera A, Epel BL. Subcellular dynamics and role of *Arabidopsis* β-1,3-glucanases in cell-to-cell movement of tobamoviruses. Mol Plant Microbe Interact. 2013:**26**(9):1016–1030. https://doi.org/10.1094/MPMI-03-13-0062-R

Zwieniecki MA, Brodribb TJ, Holbrook NM. Hydraulic design of leaves: insights from rehydration kinetics. Plant Cell Environ. 2007:**30**(8):910–921. https://doi.org/10.1111/j.1365-3040.2007.001681.x